Downloaded from http://rspb.royalsocietypublishing.org/ on November 17, 2017

PROCEEDINGS OF THE ROYAL SOCIETY B

FirstCite® e-publishing

Proc. R. Soc. B
doi:10.1098/rspb.2010.2179
Published online

Flight in slow motion: aerodynamics of the pterosaur wing

Colin Palmer*

Department of Earth Sciences, University of Bristol, Bristol, UK

The flight of pterosaurs and the extreme sizes of some taxa have long perplexed evolutionary biologists. Past reconstructions of flight capability were handicapped by the available aerodynamic data, which was unrepresentative of possible pterosaur wing profiles. I report wind tunnel tests on a range of possible pterosaur wing sections and quantify the likely performance for the first time. These sections have substantially higher profile drag and maximum lift coefficients than those assumed before, suggesting that large pterosaurs were aerodynamically less efficient and could fly more slowly than previously estimated. In order to achieve higher efficiency, the wing bones must be faired, which implies extensive regions of pneumatized tissue. Whether faired or not, the pterosaur wings were adapted to low-speed flight, unsuited to marine style dynamic soaring but adapted for thermal/slope soaring and controlled, low-speed landing. Because their thin-walled bones were susceptible to impact damage, slow flight would have helped to avoid injury and may have contributed to their attaining much larger sizes than fossil or extant birds. The trade-off would have been an extreme vulnerability to strong or turbulent winds both in flight and on the ground, akin to modern-day paragliders.

Keywords: flight; wing membrane; pterosaurs; aerodynamics

1. INTRODUCTION

Pterosaurs were flying reptiles that lived alongside the dinosaurs throughout most of the Mesozoic (*ca* 220–65 Ma) [1]. Unlike their living functional counterparts, birds and bats, pterosaurs possessed a flexible, membranous wing that was supported by a single, super-elongate wing finger [1–3]. As far as is known, no other flying vertebrates have ever adopted this gross morphology and there are no direct analogues in mechanical aerodynamics, the closest being the mainsail of a sailboat [4].

Although we know from fossils with preserved soft tissues that the pterosaur wing membrane was thin (most likely of varying elasticity), with internal reinforcing fibres—perhaps surface fibres (pycnofibres) [3]—and possibly pneumatized in the regions closest to the wing bones [5], it remains difficult to determine the nature of the membrane attachment to the bony skeleton. It was probably either midway between the dorsal and ventral sides of the wing bones [6], as in bats [7], or attached entirely to their dorsal surfaces [8].

Reconstructions of pterosaur flight capabilities have varied hugely because of structural and biomechanical unknowns (e.g. [9–17]). Most have been based on assumptions of wing bone morphology from fossil evidence, combined with wing section data drawn from the pre-1950s aerodynamic literature, which are necessarily unrepresentative of actual pterosaur wing profiles. Results from more recent theoretical and experimental work on low-speed aerofoils [18] and sail boats [19,20] can improve our understanding of the relevant airflow phenomena (see electronic supplementary material), but still do not provide results that can be directly applied to possible pterosaur wing sections. Only two specific investigations [11,21] of such sections have been published, but both contain anomalous results (see electronic supplementary material). Consequently, it is not possible to quantify the effects of varying the location of the wing bone relative to the lifting surface, varying the camber of the wing section or of different wing bone cross-sections. In the absence of such data it is not possible to predict the overall flight performance with any certainty. To address this deficit, two-dimensional models of a range of wing sections were made and tested in a low-speed wind tunnel and the results used to produce comparative flight performance curves for large, generic ornithocheiridomorph (Pteranodontidae, Istiodactylidae, Anhangueridae, etc.) pterosaurs. The sources of information are described in more detail in the electronic supplementary material, but the models were made intentionally generic so that the results would be widely applicable and not species-specific.

2. METHODS

(a) *Model tests*

Two-dimensional rigid and flexible models of wing sections representative of different cross-section locations (figure 1) along the wing of a generic, 5.8-m-wingspan derived pterosaur were constructed and tested in a wind tunnel at appropriate values of Reynolds number (*Re*; see electronic supplementary material). The rigid models were made from thin, curved sheets of epoxy resin/carbon fibre composite (figure 2). Since the actual camber of the pterosaur wing membranes cannot be known with any precision, models were made with three different camber values to provide a range of results. Pterosaur wings comprised two distinct regions—the proximal region where a propatagium was present and the distal region where it was absent [1,2]. The distal region of the main wing membrane was supported by wing bones situated along the anterior margin, whereas in

*colin.palmer@bristol.ac.uk

Electronic supplementary material is available at http://dx.doi.org/10.1098/rspb.2010.2179 or via http://rspb.royalsocietypublishing.org.

Received 8 October 2010
Accepted 3 November 2010

This journal is © 2010 The Royal Society

Downloaded from http://rspb.royalsocietypublishing.org/ on November 17, 2017

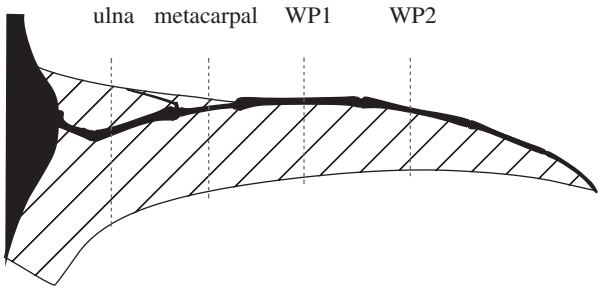

Figure 1. Generalized shape of the wing of a large ornithocheirid pterosaur. Redrawn from recent reconstructions [16,17,46], and showing the locations of the wing sections that were tested and the extent of the wing membrane assumed (cross-hatched area).

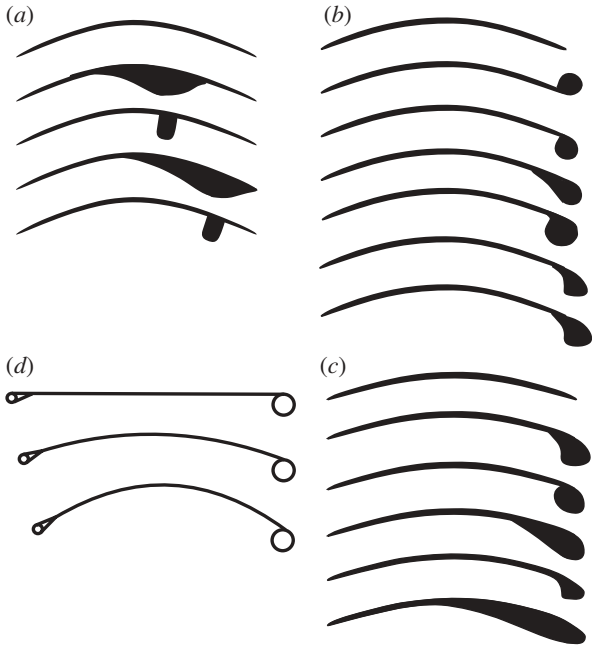

Figure 2. Wing sections that were tested. (*a*) High-camber (14.6%) proximal region with ulna faired and unfaired, 20% and 40% of chord from anterior margin. (*b*) Medium-camber (11.5%) section representing central region of the wing fitted with WP1 and WP2 phalanx sections of two different sizes (nominally with depth of 7.5% and 10% of section chord) fitted on ventral side of the wing section. The WP1 section was also tested on the dorsal side and with a small aerodynamic fairing [8]. (*c*) Low-camber section (8.5%) fitted with WP1 and WP2 sections. WP1 section faired according to Padian & Rayner [8] and WP2 section faired to the least extent required to minimize separation, as predicted from XFOIL analysis [47]. (*d*) Flexible section with three different degrees of slackness (in the unloaded condition—the actual camber increased with aerodynamic load).

the proximal region the wing bones lay within the margins of the membrane (figure 1). The local width of the propatagium depends upon the assumed angle of the elbow joint, and orientation and point of location of the pteroid. The proximal region was therefore modelled with the wing bone (ulna) on the ventral side at 20 and 40 per cent of the wing chord from the anterior margin, to represent different propatagium width reconstructions. Faired and unfaired geometries were used to model possible muscle tissue. The first wing phalanx (WP1) was modelled with oval sections of two different sizes,

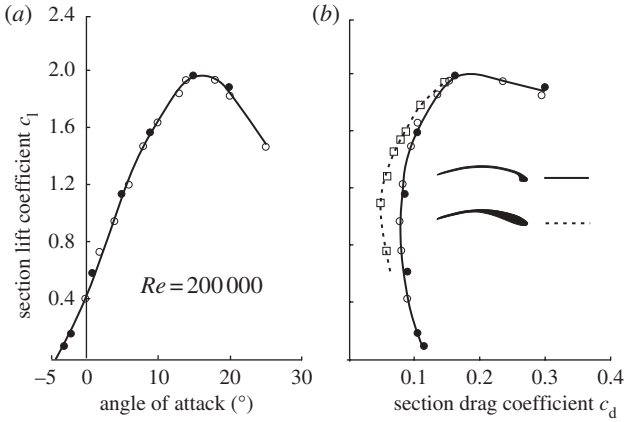

Figure 3. Typical wind tunnel test results at $Re = 200\,000$. (*a*) Variation of section lift coefficient (c_l) with angle of attack for WP2 wing bone section. Open circles: results with increasing angle of attack. Filled circles: results for decreasing angle of attack. The closeness of these results demonstrates good test repeatability and absence of hysteresis effects. (*b*) Effect of section fairing on $c_l : c_d$ for the WP2 wing section. The extensive fairing significantly reduces the minimum drag coefficient but has no effect on maximum lift coefficient.

with and without a soft tissue fairing on its posterior face [8]. The second wing phalanx (WP2) models were subtriangular in section. One was faired extensively.

The membrane of the flexible model was made from latex rubber, reinforced in the proximodistal direction with thin cotton fibres to represent the anisotropic properties of the membrane conferred by internal reinforcing fibres [3,22]. The membrane elasticity was scaled to be equivalent to 2-mm-thick skin with the same properties as bat wings [23]. The posterior edge of the membrane could be moved in the anteroposterior direction to change the slackness in the membrane, and thus its camber. Three locations were tested, giving 0, 9.5 and 18 per cent camber when slack. All the results were corrected for wind-tunnel-blockage effects [24].

To validate the tests, the cambered plate model results were compared with results published by Milgram [25], the only comprehensive data available for thin cambered plate aerofoils at low *Re* (<500 000) over a range of camber ratios. The overall shape and trends of the results were very similar, giving confidence that the results being reported here are reliable. Detailed differences are probably owing to differences between the section shapes and characteristics of the air flow in the wind tunnels, well-known problems when results are compared between facilities [26,27]. These differences do not invalidate detailed comparisons between the results obtained in the same test facility or more general comparisons across facilities.

(b) *Analysis of results*

Results were analysed by reference to the relationships between c_l and c_d (section lift coefficient and drag coefficient). One typical set of results is shown in figure 3. In order to compare and quantify the effects of the different wing section characteristics, the lift : drag relationships were used to calculate the flight performance of a notional three-dimensional pterosaur with a wing area of 2.2 m^2, wingspan of 5.8 m and mass ranging between 13.9 and 32 kg [10,12,28,29], using the standard techniques of aircraft design [30]. The drag was calculated as the sum of the profile drag measured

Downloaded from http://rspb.royalsocietypublishing.org/ on November 17, 2017

in the two-dimensional tests, the parasitic drag of the body and the induced drag (drag owing to lift). The resulting lift and drag values were then used to calculate a glide polar curve (the variation of sink speed with forward speed [31,32]).

The parasitic drag of the body was calculated using the methodology of Bramwell & Whitfield [10] in order that comparisons could be made with their work. The induced drag was calculated using the standard aerodynamic formulation [30]: $C_{\mathrm{Di}} = C_{\mathrm{L}}^2/(e\pi AR)$, where e is a constant dependent upon the geometry of the wing planform, AR the aspect ratio of the wings and C_{L} the wing lift coefficient. A value of $e = 0.9$ was used, applicable to a highly tapered wing [4]. AR was calculated from $AR = B^2/S$ (where $B =$ the total wing span and S the wing area).

The polar curve was calculated using the identity $C_{\mathrm{T}} = W/(0.5\rho S V_{\mathrm{a}}^2)$, where C_{T} is the resultant of C_{L} and C_{D} (the wing lift and drag coefficients), W the weight of the animal, ρ the mass density of air and V_{a} the airspeed. This is solved to give the airspeed vector, from which the horizontal and vertical speed components can be derived.

The resultant curve is an inverted U shape, and the maximum of the curve is the point of minimum sink. The point where it is tangential to a line through the axis is the maximum aerodynamic efficiency (L/D_{max}) and also the maximum range in still air. It is important to be aware of this distinction. At minimum sink, time in the air is maximized, whereas at L/D_{max} the range is maximized. The former matters more for behaviour that relies on soaring in rising air [31]. Minimum sink can be improved in two ways: by increasing the L/D_{max} and/or by reducing the flight speed, as moving towards the top left of the graph improves the sink rate without an increase in aerodynamic efficiency. Indeed, it is possible to improve minimum sink even as L/D_{max} reduces.

One other region of the polar curve deserves attention—the bottom left of the graph. This is where speed becomes very low and flight can only be sustained by achieving high values of lift coefficient. A precipitous drop in the polar curve reflects a sudden stall and probable loss of control. A more rounded shape reflects a more gradual and controlled transition from flight to stall.

3. RESULTS

The ulna positioned at 40 per cent of wing chord (faired or unfaired) reduced maximum lift but did not increase minimum drag, resulting in only a small reduction in aerodynamic efficiency. A more anterior (20% chord) location for this wing bone resulted in a greater reduction in performance, but in both cases the effect of the fairing was very small.

Tests with the WP1 and WP2 phalanges gave the following results. (i) With the sections on the ventral side, drag increased substantially (when compared with a cambered section alone), with little difference between the two shapes. There was almost no effect on the maximum lift (in fact it increased a little with the WP2 phalanx). (ii) A phalanx located on the dorsal side of the wing reduced the section performance substantially, increasing drag and decreasing the maximum lift coefficient. (iii) The larger the bone section relative to the width of the wing section, the greater the drag. (iv) Fairing the phalanx sections to the extent previously suggested [8] did not reduce the drag or influence the maximum lift. (v) A more extensive fairing, designed to minimize separation, reduced the drag by 35 per cent with no change in maximum lift. (vi) The flexible section had similar minimum drag but greatly increased maximum lift (>25%) (at the cost of high drag). (vii) The maximum lift coefficients produced by the rigid sections approached 2.0 and were still higher for the flexible section, values considerably in excess of those reported for birds [32,33].

4. DISCUSSION

Pterosaur wing section performance is sensitive to wing bone location and size because the bones trigger flow separation (which creates drag) but this effect is reduced when they are positioned posterior to the wing margin (on the ventral side). The humerus and ulna are the largest-diameter bones in the pterosaur wing and would have been surrounded by soft tissue, further increasing their size; so proximal regions of the wing would have potentially suffered substantial loss of performance owing to these bones. However, this effect was mitigated by the propatagium, which positioned the bones posterior to the anterior margin of the membrane, and so acted as a drag reduction device (*contra* [21]). Such a thin leading edge section is very sensitive to the local angle of incident flow [34], which might explain the role of the pterosaur pteroid—to vary the local incidence angle of the propatagium as the overall angle of attack of the wing changed, and thus maintain the optimum flow conditions.

When a phalanx was positioned on the anterodorsal wing margin, the performance was highly degraded. Similar results have been seen in sail/mast tests [20,35,36], together providing strong support for ventral wing finger positioning [8].

The glide polars constructed from these wing section results show the influences on the overall flight performance (figure 4). Flight efficiency is significantly inferior to previous estimates [10,12], and somewhat lower than some extant soaring birds [37–40]. However, owing to the low flight speed, the minimum sink rate (approx. $1.0\ \mathrm{m\ s^{-1}}$) was comparable to extant birds [32,37–40] and bats [41]. As wing bone size increases (relative to the wing chord), the sink rate increases with little effect upon flight speed.

The flight performance was improved by extensive fairing of the wing bones, and, while the presence of such a fairing is entirely speculative, it may have been provided by pneumatized tissue [5]. The fairing increased the aerodynamic efficiency and flight speed, but had only a limited effect upon the minimum sink speed, the parameter that determines the loitering and thermal/slope soaring capability.

With a flexible membrane, the flight envelope was extended to lower speeds owing to the enhanced high lift capability and progressive stall of these sections. Since the animals presumably had some control over the wing camber [3,22], the envelope curve around the results with the flexible membrane best shows the full range of performance. When compared with the rigid wing section results, the low-speed flight capability is extended and combined with a softer stall, which would have enhanced control during landing manoeuvres when low speed, high drag and high lift are required.

In conclusion, these tests have quantified the two-dimensional characteristics of possible pterosaur wing

Downloaded from http://rspb.royalsocietypublishing.org/ on November 17, 2017

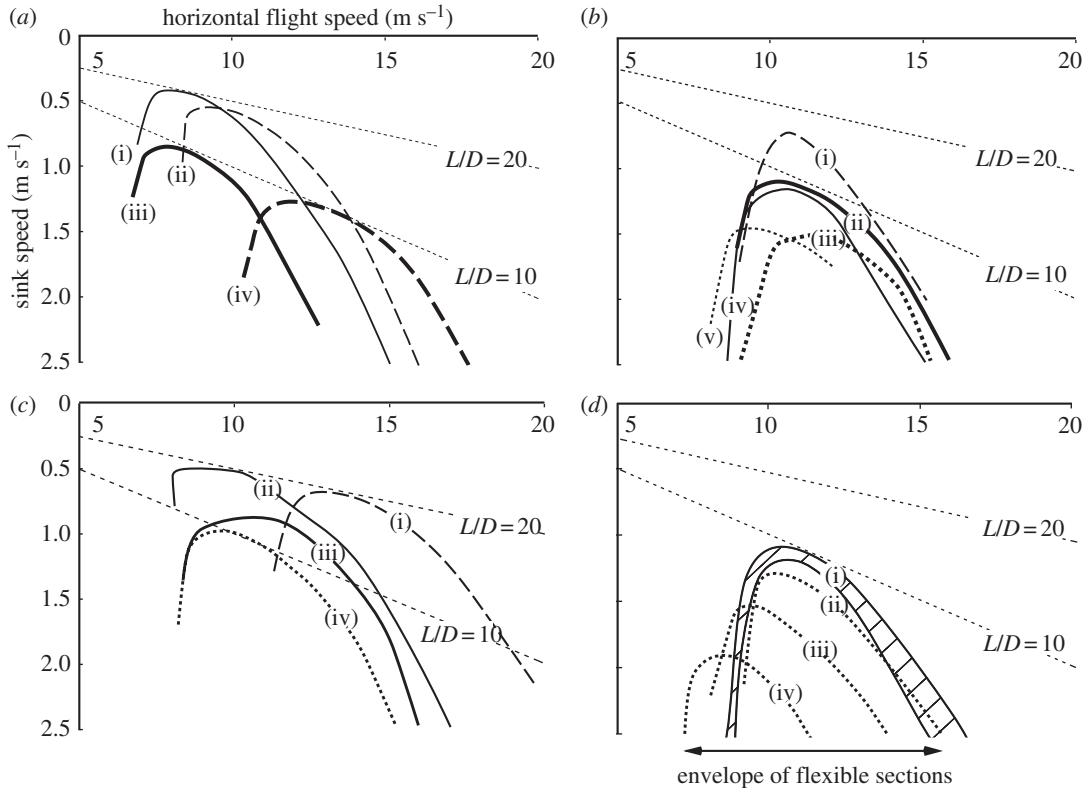

Figure 4. Polar glide curves. (*a*) Comparison with results from previous studies ((i) [10]; (ii) [12]), with results from present tests (WP1 medium camber section) at two extremes of mass ((iii) and (iv)). The WP1 wing has only half the aerodynamic efficiency (*L*/*D* ratio) and almost twice the sink rate of the earlier estimates. (*b*) Effect of different wing bone sizes and shapes: (i) section with no bone; (ii) small WP1; (iii) large WP1; (iv) small WP2; and (v) large WP2. The WP1 phalanges move the polar curve downwards with increasing size, resulting in little change in the optimum flight speed but a large increase in the sink rate. The WP2 phalanges have similar effects, but because they increase both drag and the maximum lift coefficient, the glide polar moves a little to the left, extending the low-speed flight envelope. (*c*) Potential performance of an optimized wing section: (i) 417a section used in earlier reconstructions; (ii) optimized modern S1223 laminar flow aerofoil section [48]; (iii) WP2 faired with XFOIL designed fairing; and (iv) small WP2 only. The two aerofoil sections give similar peak efficiencies of 20 : 1, but the S1223 section maintains good performance to higher values of lift coefficient, shifting the polar curve to the left. (*d*) Effect of flexibility: (i) envelope of rigid sections with same bone depth as flexible section, and (ii)–(iv) the flexible section with increasing membrane slackness.

sections for the first time. They show that these creatures were significantly less aerodynamically efficient and more capable of flying at lower speeds than previously estimated. In order to achieve higher efficiency, the wing bones must be faired, which either implies a substantial weight penalty owing to the additional tissue required or, more likely, a high degree of pneumaticity in the fairing tissue.

Whether faired or not, the pterosaur wing sections were adapted to a low-speed flight regime that minimizes the sink rate. This regime is unsuited to marine-style dynamic soaring adopted by procellariiform birds, which requires high flight speed coupled with high aerodynamic efficiency [42,43], but is well suited to thermal/slope soaring. The low sink rate would have allowed pterosaurs to use the relatively weak thermal lift found over the sea [44,45]. Since the bones of pterosaurs were thin-walled and consequently very susceptible to impact damage, the low-speed landing capability would have made an important contribution to avoiding injury, and so helped to enable pterosaurs to attain much larger sizes than extant birds. Indeed, the maximum lift capability of a pterosaur wing was substantially higher than in birds, enabling slow flight and mitigating the allometric constraint on size that manifests in the fast landing speeds of large extant birds. The trade-off for pterosaurs would have been extreme vulnerability to strong winds and turbulence, not unlike modern-day paragliders.

I am grateful to G. Dyke, M. Benton, E. Rayfield, P. Gill and two anonymous reviewers for their helpful comments on earlier drafts of this manuscript, and to Malachy O'Rourke for the use of the UCD School of Electrical, Electronic and Mechanical Engineering wind tunnel.

REFERENCES

1 Wellnhofer, P. 1991 *The illustrated encyclopedia of pterosaurs*. London, UK: Salamander.
2 Unwin, D. M. 2005 *The pterosaurs: from deep time*. New York, NY: Pi Press.
3 Kellner, W. A., Wang, X., Tischlinger, H., Campos, D., Hone, D. W. E. & Meng, X. 2009 The soft tissue of *Jeholopterus* (Pterosauria, Anurognathidae, Batrachognathinae) and the structure of the pterosaur wing membrane. *Proc. R. Soc. B* **277**, 321–329. (doi:10.1098/rspb.2009.0846)
4 Marchaj, C. A. 1979 *Aero-hydrodynamics of sailing*. London, UK: Adlard Coles Nautical.
5 Claessens, L. P. A. M., O'Connor, P. M. & Unwin, D. M. 2009 Respiratory evolution facilitated the origin of pterosaur flight and aerial gigantism. *PLoS ONE* **4**, e4497. (doi:10.1371/journal.pone.0004497)

Downloaded from http://rspb.royalsocietypublishing.org/ on November 17, 2017

6 Frey, E. & Riess, J. 1981 A new reconstruction of the pterosaur wing. *N. Jb. Geol. Paläont. Abh.* **161**, 1–27.
7 Norberg, U. M. L. 2002 Structure, form, and function of flight in engineering and the living world. *J. Morphol.* **252**, 52–81. (doi:10.1002/jmor.10013)
8 Padian, K. & Rayner, J. M. V. 1993 The wings of pterosaurs. *Am. J. Sci.* **293**, 91–166. (doi:10.2475/ajs.293.A.91)
9 Hankin, E. H. & Watson, D. M. S. 1914 On the flight of pterodactyls. *Aero. J.* **18**, 24–335.
10 Bramwell, C. D. & Whitfield, G. R. 1974 Biomechanics of *Pteranodon*. *Phil. Trans. R. Soc. Lond. B* **267**, 503–581. (doi:10.1098/rstb.1974.0007)
11 Stein, R. S. 1975 Dynamic analysis of *Pteranodon ingens*: a reptilian adaptation for flight. *J. Paleont.* **49**, 534–548.
12 Brower, J. C. 1983 The aerodynamics of *Pteranodon* and *Nyctosaurus*, two large Pterosaurs from the Upper Cretaceous of Kansas. *J. Vert. Paleont.* **3**, 84–124. (doi:10.1080/02724634.1983.10011963)
13 Pennycuick, C. J. 1988 On the reconstruction of pterosaurs and their manner of flight, with notes on vortex wakes. *Biol. Rev.* **63**, 209–231. (doi:10.1111/j.1469-185X.1988.tb00633.x)
14 Hazlehurst, G. 1991 The morphometric and flight characteristics of the Pterosauria. PhD thesis, University of Bristol, Bristol, UK.
15 Frey, E., Buchy, M.-C. & Martill, D. M. 2003 Middle- and bottom-decker Cretaceous pterosaurs: unique designs in active flying vertebrates. In *Evolution and palaeobiology of pterosaurs* (eds E. Buffetaut & J.-M. Mazin), pp. 267–274. Special Publications 217. London, UK: Geological Society of London.
16 Wilkinson, M. T. 2008 Three-dimensional geometry of a pterosaur wing skeleton, and its implications for aerial and terrestrial locomotion. *Zool. J. Linn. Soc.* **154**, 27–69. (doi:10.1111/j.1096-3642.2008.00409.x)
17 Bennett, S. C. 2007 Articulation and function of the pteroid bone of pterosaurs. *J. Vert. Paleo.* **27**, 881–891. (doi:10.1671/0272-4634(2007)27[881:AAFOTP]2.0.CO;2)
18 Shyy, W., Lian, Y., Tang, J., Viieru, D. & Liu, H. 2008 *Aerodynamics of low Reynolds number flyers*. Cambridge, UK: Cambridge University Press.
19 Marchaj, C. A. 1996 *Sail performance: theory and practice*. London, UK: Adlard Coles Nautical.
20 Chapin, V. G., Jamme, S. & Chassaing, P. 2005 Viscous computational fluid dynamics as a relevant decision-making tool for mast-sail aerodynamics. *Mar. Technol. Soc. J.* **42**, 1–10.
21 Wilkinson, M. T., Unwin, D. M. & Ellington, C. P. 2006 High lift function of the pteroid bone and forewing of pterosaurs. *Proc. R. Soc. B* **273**, 119–126. (doi:10.1098/rspb.2005.3278)
22 Bennett, S. C. 2000 Pterosaur flight: the role of actinofibrils in wing function. *Hist. Biol.* **14**, 255–284. (doi:10.1080/10292380009380572)
23 Swartz, S. M., Groves, M. S., Kim, H. D. & Walsh, W. R. 1996 Mechanical properties of bat wing membrane skin. *J. Zool. Soc. Lond.* **239**, 357–378. (doi:10.1111/j.1469-7998.1996.tb05455.x)
24 Barlow, J. B., Rae, W. H. & Pope, A. 1999 *Low speed wind tunnel testing*, 3rd edn. New York, NY: Wiley Interscience.
25 Milgram, J. H. 1971 Section data for thin, highly cambered airfoils in incompressible flow. Report CR-1767. Washington, DC: National Aeronautics and Space Administration.
26 Hoerner, S. F. 1985 *Fluid-dynamic lift*. NJ, USA: Hoerner Fluid Dynamics.
27 NACA 1921 Aerodynamic characteristics of aerofoils. Report no. 93, National Advisory Committee for Aeronautics. See http://naca.central.cranfield.ac.uk/reports/1921/naca-report-93.pdf.
28 Witton, M. T. 2009 A new approach to determining pterosaur body mass and its implications for pterosaur flight. In *Flugsaurier: pterosaur papers in honour of Peter Wellnhofer. Zitteliana Series B* (*special volume*) (eds E. Buffetaut & D. W. E. Hone), vol. 28, pp. 143–159.
29 Henderson, D. M. 2010 Pterosaur body mass estimates from three-dimensional mathematical slicing. *J. Vert. Paleo.* **30**, 768–785. (doi:10.1080/02724631003758334)
30 Anderson, J. D. 2007 *Fundamentals of aerodynamics*. New York, NY: McGraw-Hill International.
31 Vogel, S. 1994 *Life in moving fluids: the physical biology of flow*. Princeton, NJ: Princeton University Press.
32 Azuma, A. 2006 *The biokinetics of flying and swimming*, 2nd edn. Reston, VA: AIAA Education Series.
33 Pennycuick, C. J. 1983 Thermal soaring compared in three dissimilar tropical bird species, *Fregata magnificens*, *Pelecanus occidentalis* and *Coragyps atratus*. *J. Exp. Biol.* **102**, 307–325.
34 Shyy, W., Berg, M. & Ljunqvist, D. 1999 Flapping and flexible wings for biological and micro air vehicles. *Progr. Aerospace Sci.* **35**, 455–506. (doi:10.1016/S0376-0421(98)00016-5)
35 Garrett, R. 1987 *The symmetry of sailing: the physics of sailing for yachtsmen*. London, UK: Adlard Coles.
36 Paton, J. S. & Morvan, H. P. 2007 The effect of mast rotation and shape on the performance of sails. *Int. J. Mar. Eng.* **149**. (doi:10.3940/rina.ijme.2007.a2.10307)
37 Tennekes, H. 1997 *The simple science of flight: from insects to jumbo jets*. Cambridge, MA: MIT Press.
38 Alexander, R. M. 2003 *Principles of animal locomotion*. Princeton, NJ: Princeton University Press.
39 Pennycuick, C. J. 2008 *Modelling the flying bird*. Theoretical Ecology Series. The Netherlands: Academic Press, Elsevier Inc.
40 Pennycuick, C. J. 1971 Gliding flight of the white-backed vulture *Gyps africanus*. *J. Exp. Biol.* **55**, 13–38.
41 Pennycuick, C. J. 1971 Gliding flight of the dog-faced bat *Rousettus aegyptiacus* observed in a wind tunnel. *J. Exp. Biol.* **55**, 833–845.
42 Sachs, G. 2005 Minimum shear wind strength required for dynamic soaring of albatrosses. *Ibis* **147**, 1–10. (doi:10.1111/j.1474-919x.2004.00295.x)
43 Lissaman, P. 2005 Wind energy extraction by birds and flight vehicles. AIAA paper 2005-241. Reston, VA: American Institute for Aeronautics and Astronautics.
44 Woodcock, A. H. 1975 Thermals over the sea and gull flight behaviour. *Boundary-Layer Meteorol.* **9**, 63–68. (doi:10.1007/BF00232254)
45 Agee, E. M. & Sheu, P. J. 1977 MCC and gull flight behaviour. *Boundary-Layer Meteorol.* **14**, 247–251. (doi:10.1007/BF00122622)
46 Palmer, C. & Dyke, G. 2009 Biomechanics of the unique pterosaur pteroid. *Proc. R. Soc. B* **277**, 1121–1127. (doi:10.1098/rspb.2009.1899)
47 Drela, M. & Giles, M. B. 1987 Viscous-inviscid analysis of transonic and low Reynolds number airfoils. *AIAA J.* **25**, 1347–1355. (doi:10.2514/3.9789)
48 Selig, M. S. & Gulielmo, J. J. 1977 High-lift low Reynolds number airfoil design. *J. Air.* **34**, 72–79. (doi:10.2514/2.2137)